Beyond the Design Point: When Equal Failure Probabilities May Not Be Equal

Marco Broccardo and Johannes O. Royset

[1)] *Department of Civil, Environmental and Mechanical Engineering, University of Trento, 38132 Trento, Italy - marco.broccardo@unitn.it*

[2)] *Daniel J. Epstein Department of Industrial and Systems Engineering, University of Southern California, CA 90089 Los Angeles, USA - royset@usc.edu*

Abstract. In structural reliability, the probability of failure and the associated reliability index are usually treated as complete summaries of structural safety. This convention is powerful, but it hides an important distinction: two systems may have the same failure probability while exhibiting markedly different failure mechanisms and tail severities. This paper revisits the role of the classical design point and proposes two complementary quantities for interpreting failure beyond its probability. The first is the Mean Failure Point, a representative point in the standard normal space associated with the expected performance conditional on failure. It characterizes where the failure event is expected to lie, rather than where the limit-state surface is most likely to be reached. The second is the Buffered Reliability Index, obtained from the buffered probability of failure, which incorporates the tail behavior of the performance function. In the linear standard normal case, both quantities admit closed-form expressions involving the hazard rate of the standard normal distribution, clarifying their relation with the classical reliability index. The resulting triplet—failure probability, Mean Failure Point, and Buffered Reliability Index—offers a compact description of how likely failure is, how it occurs, and how severe it may be.

Keywords: structural reliability, design point, reliability index, buffered probability of failure, superquantile, failure mechanism

1. Introduction

The design point is one of the central concepts of structural reliability. In the standard normal space, it is defined as the point on the limit-state surface that lies closest to the origin. Equivalently, under the usual regularity assumptions, it identifies the location at which the transformed joint density is largest among the points that satisfy the limit-state equation. This point provides the geometric foundation of the Hasofer–Lind reliability index (Hasofer and Lind, 1974) and of the First- and Second-Order Reliability Methods, FORM and SORM (Breitung, 1984; Der Kiureghian et al., 1987). It is also the point around which many asymptotic and simulation-based approximations of rare failure events are organized. The appeal of the design point is not only computational. It provides a concise geometric interpretation of safety. A structure is regarded as safer when the limit-state surface is farther from the origin in the standard normal space. This interpretation has deeply influenced modern reliability theory and the calibration of partial safety factors in design codes. There is, however, an important limitation. The classical formulation tells us how likely it is that a structure reaches the failure domain, but it says little about how the failure develops once the domain is entered. The design point lies on the boundary of failure. It is therefore a boundary descriptor, not a descriptor of the interior of the failure domain. As a consequence, two systems may have the same probability of failure, and even equal design-point distances, while exhibiting very different failure mechanisms. One system may enter the failure domain only mildly, another may enter a deep tail region. This distinction matters because engineering design is rarely concerned with failure probability alone. The historical evolution from allowable-stress design to load-factor design and performance-based design reflects a broader objective: not only to avoid failure, but also to control the mode and consequences of failure. A ductile and observable failure mechanism is not equivalent to a brittle and sudden one, even when both mechanisms have the same nominal probability of occurrence. The statement "equal failure probabilities imply equal reliability" is therefore too narrow when reliability is interpreted as a physical property of a structural system.

This paper expands on ideas from (Broccardo and Royset, 2025) of the classical framework. The key idea is to supplement the failure probability with information about the conditional distribution of the performance function within the failure domain. Two quantities are introduced. The first is the Mean Failure Point (MFP), a representative point in the standard normal space associated with the conditional expected failure level. The MFP is intended to describe the typical location and direction of failure beyond the limit-state surface. The second is the Buffered Reliability Index (BRI), a tail-dependent reliability index derived from the buffered probability of failure (Rockafellar and Royset, 2010). While the classical reliability index is equivalent to the failure probability, the BRI also responds to the severity and spread of the adverse tail. The proposed view is summarized by augmenting the single reliability descriptor $P_{\mathcal{F}}$ or β with the triplet

$$\left(P_{\mathcal{F}},\, \boldsymbol{z}^{**},\, \underline{\beta}\right), \tag{1}$$

where $P_{\mathcal{F}}$ is the probability of failure, $\boldsymbol{z}^{**}$ is the MFP, and $\underline{\beta}$ is the BRI. The first term measures likelihood, the second identifies a representative failure configuration, and the third accounts for tail severity. The aim is not to discard the design point, but to place it within a broader reliability description that is more consistent with the mechanics of failure.

2. Classical reliability and the design point

Let the performance of a structural system be described by a limit-state function

$$Y = g(\boldsymbol{X}), \qquad \boldsymbol{X} \in \mathbb{R}^n, \tag{2}$$

where $Y \leq 0$ defines failure and $Y > 0$ defines safety. If $\boldsymbol{X}$ has joint density $f_{\boldsymbol{X}}(\boldsymbol{x})$, the probability of failure is

$$P_{\mathcal{F}} = \mathbb{P}[Y \leq 0] = \int_{\mathbb{R}^n} \mathbf{1}\{g(\boldsymbol{x}) \leq 0\} f_{\boldsymbol{X}}(\boldsymbol{x})\, \mathrm{d}\boldsymbol{x}. \tag{3}$$

More generally, the distribution of Y is

$$F_Y(y) = \mathbb{P}[Y \le y] = \int_{\mathbb{R}^n} \mathbf{1}\{g(\boldsymbol{x}) \le y\} f_{\boldsymbol{X}}(\boldsymbol{x})\,\mathrm{d}\boldsymbol{x}, \tag{4}$$

so that $P_{\mathcal{F}} = F_Y(0)$. Through an isoprobabilistic transformation $\boldsymbol{z} = \mathcal{T}(\boldsymbol{x})$, the problem is mapped to the standard normal space. The transformed vector $\boldsymbol{Z} \in \mathbb{R}^n$ has independent standard normal components and density $\varphi(\boldsymbol{z})$. With

$$G(\boldsymbol{z}) = g\big(\mathcal{T}^{-1}(\boldsymbol{z})\big), \tag{5}$$

Eq. (4) becomes

$$F_Y(y) = \int_{\mathbb{R}^n} \mathbf{1}\{G(\boldsymbol{z}) \le y\}\varphi(\boldsymbol{z})\,\mathrm{d}\boldsymbol{z}. \tag{6}$$

In the Hasofer–Lind formulation (Hasofer and Lind, 1974), the design point is obtained as

$$\boldsymbol{z}^* \in \arg\min_{\boldsymbol{z}} \left\{ \|\boldsymbol{z}\|_2^2 \;\middle|\; G(\boldsymbol{z}) = 0 \right\}. \tag{7}$$

The Hasofer–Lind reliability index, introduced to provide an invariant measure of reliability, is

$$\beta_{HL} = \|\boldsymbol{z}^*\|_2 \,. \tag{8}$$

This formulation overcame the lack of invariance of earlier reliability indices with respect to equivalent mathematical representations of the limit-state function. If G is differentiable at $\boldsymbol{z}^*$, FORM approximates the limit-state surface by its tangent hyperplane at $\boldsymbol{z}^*$ (Hasofer and Lind, 1974) and gives

$$P_{\mathcal{F}} \approx \Phi(-\beta_{HL}), \tag{9}$$

where Φ is the standard normal distribution function. SORM improves this approximation by incorporating local curvature information at the design point (Breitung, 1984; Der Kiureghian, 2022). When the actual probability of failure is known or accurately estimated, the generalized reliability index (Ditlevsen, 1979) is defined as

$$\beta = -\Phi^{-1}(P_{\mathcal{F}}). \tag{10}$$

Thus, $P_{\mathcal{F}}$ and β contain the same information. Two systems with the same $P_{\mathcal{F}}$ have the same generalized reliability index, independently of the shape of the failure domain or the distribution of the performance function below zero. This equivalence is mathematically consistent, but it is incomplete from a mechanical point of view. The design point is best understood as a descriptor of the boundary of the failure event. It identifies the most likely way to reach the limit-state surface, not the expected state of the system once failure has occurred. This distinction motivates the next section.

3. Beyond the design point: Mean Failure Point

The purpose of the Mean Failure Point is to identify a representative point within the failure domain. The guiding question is simple: conditional on failure occurring, which failure state best represents the event? The answer should not be constrained to the limit-state surface $G(\boldsymbol{z}) = 0$, because actual failure states lie in the domain $G(\boldsymbol{z}) \leq 0$.

3.1. Conditional expected failure level

Since the performance Y is a random variable, the most natural scalar representative of the failure outcome under squared-error loss is the conditional mean

$$\underline{y} = \arg\min_{y \in \mathbb{R}} \mathbb{E}\left[(Y - y)^2 \mid Y \leq 0\right] = \mathbb{E}[Y \mid Y \leq 0]. \tag{11}$$

The notation $\underline{y}$ emphasizes that, except in degenerate cases, this value is negative. It is the expected performance level conditional on failure, and therefore depends on the tail of the distribution of Y below zero.

The value $\underline{y}$ defines a new level set,

$$\Sigma_{\underline{y}} = \left\{ \boldsymbol{z} \in \mathbb{R}^n \,\middle|\, G(\boldsymbol{z}) = \underline{y} \right\}, \tag{12}$$

which lies beyond the classical limit-state surface. Points on this level set are not merely incipient failures; they correspond to the expected failure severity in the performance domain.

3.2. Definition of the Mean Failure Point

Among the points on $\Sigma_{\underline{y}}$, the representative point is defined as the intrinsic Fréchet mean of the conditional probability measure induced on $\Sigma_{\underline{y}}$ (Fréchet, 1948; Karcher, 1977). Specifically,

$$\boldsymbol{z}^{**} = \arg\min_{\boldsymbol{z}_0 \in \Sigma_{\underline{y}}} \int_{\Sigma_{\underline{y}}} d_{\Sigma_{\underline{y}}}(\boldsymbol{z}_0, \boldsymbol{z})^2 \, d\mu_{\underline{y}}(\boldsymbol{z}), \tag{13}$$

where $d_{\Sigma_{\underline{y}}}(\cdot, \cdot)$ denotes the geodesic distance on the manifold $\Sigma_{\underline{y}}$ and

$$d\mu_{\underline{y}}(\boldsymbol{z}) = \frac{\dfrac{\phi(\boldsymbol{z})}{\|\nabla G(\boldsymbol{z})\|} \, d\Sigma_{\underline{y}}(\boldsymbol{z})}{\displaystyle\int_{\Sigma_{\underline{y}}} \frac{\phi(\boldsymbol{z})}{\|\nabla G(\boldsymbol{z})\|} \, d\Sigma_{\underline{y}}(\boldsymbol{z})}. \tag{14}$$

The measure in Eq. (14) follows from the co-area formula and represents the conditional Gaussian probability distribution restricted to the level set $\Sigma_{\underline{y}}$. Unlike the conditional Euclidean mean, the intrinsic Fréchet mean is constrained to the manifold itself,

$$\boldsymbol{z}^{**} \in \Sigma_{\underline{y}}, \tag{15}$$

thereby ensuring mechanical and geometric consistency with the prescribed failure level. The corresponding point in the original space is obtained through the inverse transformation,

$$\boldsymbol{x}^{**} = \mathcal{T}^{-1}(\boldsymbol{z}^{**}). \tag{16}$$

Equation (13) defines the Mean Failure Point. It differs from the design point in two fundamental ways. First, it is associated with the conditional failure domain rather than only with the onset of failure. Second, it reflects the expected severity of failure through the level $\underline{y}$. The design point describes the most likely transition into failure, whereas the MFP characterizes a representative state within the failure domain once failure has occurred. The vector

$$\Delta\boldsymbol{z} = \boldsymbol{z}^{**} - \boldsymbol{z}^{*} \tag{17}$$

provides a compact geometric descriptor of the transition from incipient failure to expected failure. Its norm quantifies how deeply the system is expected to penetrate into the failure domain, while its direction identifies the dominant trajectory of failure development in the standard normal space. This vector may therefore be interpreted as a probabilistic-mechanical descriptor of the failure mechanism.

The exact computation of Eq. (13) is generally challenging because it requires optimization on a nonlinear manifold equipped with a geodesic metric. For regular and sufficiently concentrated level sets, a practical approximation can be obtained by replacing the intrinsic Fréchet mean with the mode of the same conditional distribution. This leads to

$$\boldsymbol{z}^{**} \simeq \arg\min_{\boldsymbol{z}} \left\{ \|\boldsymbol{z}\|_2^2 \;\middle|\; G(\boldsymbol{z}) = \underline{y} \right\}. \tag{18}$$

The optimization has the same structure as the classical design-point problem, but is performed on a deeper level set corresponding to the expected failure severity. This approximation preserves compatibility with existing reliability algorithms while providing a representative point within the failure domain.

3.3. Linear standard normal case

The linear standard normal case clarifies the relationship between the design point and the MFP. Let

$$G(\boldsymbol{Z}) = b_0 + \boldsymbol{b}^T\boldsymbol{Z}, \tag{19}$$

where $\boldsymbol{b} \neq \boldsymbol{0}$. Define

$$\beta = \frac{b_0}{\|\boldsymbol{b}\|}, \qquad \boldsymbol{\alpha} = -\frac{\boldsymbol{b}}{\|\boldsymbol{b}\|}. \tag{20}$$

Then the design point is

$$\boldsymbol{z}^{*} = \beta\boldsymbol{\alpha}. \tag{21}$$

The failure event $G(\boldsymbol{Z}) \leq 0$ is equivalent to a one-dimensional standard normal variable exceeding β in the direction $\boldsymbol{\alpha}$. By Gaussian symmetry, the MFP is collinear with the design point. Its norm is

$$\|\boldsymbol{z}^{**}\| = \mathbb{E}[Z \mid Z > \beta] = \frac{\phi(\beta)}{\Phi(-\beta)} = \lambda(\beta), \tag{22}$$

where ϕ is the standard normal density and $\lambda(\beta)$ is the standard normal hazard rate. Hence

$$\boldsymbol{z}^{**} = \lambda(\beta)\boldsymbol{\alpha}. \tag{23}$$

Since $\lambda(\beta) > \beta$ for positive β, the MFP lies beyond the design point along the same failure direction. In this special case, the mechanics of failure is one-dimensional; in nonlinear and multi-mechanism cases, the displacement from $\boldsymbol{z}^*$ to $\boldsymbol{z}^{**}$ can reveal changes in failure direction that are invisible to $P_{\mathcal{F}}$ alone.

4. Beyond the reliability index: Buffered Reliability Index

The MFP provides a representative failure configuration, but it does not by itself produce a scalar reliability index. A scalar index remains useful for comparison and communication. The question is how to define such an index so that it responds not only to the probability of crossing the limit state, but also to the severity of the adverse tail.

4.1. Tail-dependent threshold and buffered probability

We define a threshold $\bar{y}$ by imposing that the conditional mean of Y below this threshold is exactly the conventional failure level zero:

$$\mathbb{E}[Y \mid Y \leq \bar{y}] = 0. \tag{24}$$

For structural systems with positive mean safety margin and nonzero failure probability, this threshold is typically nonnegative. The corresponding probability

$$\bar{P}_{\mathcal{F}} = F_Y(\bar{y}) \tag{25}$$

is the buffered probability of failure, under continuity assumptions on the distribution of Y (Rockafellar and Royset, 2010). Because $\bar{y} \geq 0$, one has

$$\bar{P}_{\mathcal{F}} \geq P_{\mathcal{F}}. \tag{26}$$

The buffered probability is therefore conservative with respect to the classical failure probability (Rockafellar and Royset, 2010; Mafusalov and Uryasev, 2018); see (Royset, 2025) for further connections to the risk management literature broadly.

The interpretation is direct. Suppose two systems have the same value of $P_{\mathcal{F}}$. If one system has a heavier adverse tail, the conditional mean below zero is more severe. To bring the conditional mean back to zero, the threshold $\bar{y}$ must move farther into the safe side, thereby increasing $F_Y(\bar{y})$. The buffered probability therefore distinguishes systems that the classical failure probability regards as equivalent; this distinction is closely related to tail-sensitivity measures based on the ratio between buffered and classical failure probabilities (Byun and Royset, 2022).

The Buffered Reliability Index is defined as

$$\underline{\beta} = -\Phi^{-1}(\bar{P}_{\mathcal{F}}). \tag{27}$$

The underline emphasizes that

$$\underline{\beta} \leq \beta, \tag{28}$$

with equality only in limiting or degenerate cases. For two systems with the same β, the system with the heavier adverse tail has a larger $\bar{P}_{\mathcal{F}}$ and therefore a smaller $\underline{\beta}$.

In the standard normal space, Eq. (25) can be written as

$$\bar{P}_{\mathcal{F}} = \int_{\mathbb{R}^n} \mathbf{1}\{G(\boldsymbol{z}) \leq \bar{y}\}\varphi(\boldsymbol{z})\,\mathrm{d}\boldsymbol{z}. \tag{29}$$

Analogously to FORM, one may approximate $\underline{\beta}$ through the design point associated with the shifted surface $G(\boldsymbol{z}) = \bar{y}$:

$$\underline{\boldsymbol{z}}^* \in \arg\min_{\boldsymbol{z}} \left\{ \|\boldsymbol{z}\|_2^2 \;\middle|\; G(\boldsymbol{z}) = \bar{y} \right\}. \tag{30}$$

We call $\underline{\boldsymbol{z}}^*$ the Buffered Probable Point. It is not intended to replace the design point as a mechanical descriptor. Rather, it is an auxiliary point used to approximate the buffered probability and the associated BRI:

$$\underline{\beta} \approx \underline{\beta}_{HL} = \|\underline{\boldsymbol{z}}^*\|_2\,, \qquad \bar{P}_{\mathcal{F}} \approx \Phi(-\underline{\beta}_{HL}). \tag{31}$$

By construction, $\underline{\beta}_{HL} \leq \beta_{HL}$.

4.2. Linear standard normal case

For the linear model in Eq. (19), the buffered probability can be evaluated in closed form. The BRI coincides with its Hasofer–Lind approximation,

$$\bar{P}_{\mathcal{F}} = \Phi(-\underline{\beta}) = \Phi(-\underline{\beta}_{HL}). \tag{32}$$

The shifted threshold gives

$$\underline{\beta} = \frac{b_0 - \bar{y}}{\|\boldsymbol{b}\|} = \beta - \frac{\bar{y}}{\|\boldsymbol{b}\|}, \tag{33}$$

and

$$\underline{\boldsymbol{z}}^* = \underline{\beta}\,\boldsymbol{\alpha}. \tag{34}$$

The defining condition of the buffered threshold implies

$$\mathbb{E}[Z \mid Z > \underline{\beta}] = \beta, \tag{35}$$

or equivalently

$$\lambda(\underline{\beta}) = \frac{\phi(\underline{\beta})}{\Phi(-\underline{\beta})} = \beta. \tag{36}$$

Therefore,

$$\underline{\beta} = \lambda^{-1}(\beta), \tag{37}$$

and the three reliability descriptors satisfy

$$\underline{\beta} = \lambda^{-1}(\beta) \leq \beta \leq \lambda(\beta) = \|\boldsymbol{z}^{**}\|\,. \tag{38}$$

This chain is useful conceptually. The BRI lies on the safe side of the classical reliability index, while the MFP lies beyond the design point inside the failure domain. In the linear Gaussian case the three quantities are aligned; in nonlinear systems they may separate both in magnitude and direction.

5. Illustrative example: equal failure probabilities, different failure descriptions

We consider a two-variable component reliability problem in which the performance function is written in the classical resistance-minus-load form

$$g(r, s_i) = r - s_i, \qquad i = 1, 2, \tag{39}$$

so that failure occurs when the load effect exceeds the resistance, $s_i \geq r$. The resistance R is modeled as lognormal with mean 60.00 and coefficient of variation 0.15. The two load models are chosen so that they produce the same classical probability of failure, while having different distributional forms. The first load, S_1, follows a generalized extreme value distribution with parameters $\mu = 12.932$, $\sigma = 2.878$, and $\xi = 0.125$, corresponding to a Fréchet-type right tail. The second load, S_2, follows a lognormal distribution with parameters $\mu = 2.935$ and $\sigma = 0.293$. Its mean is 19.56 and its coefficient of variation is 0.30. The resistance has lognormal parameters $\mu = 4.083$ and $\sigma = 0.149$. The marginal probability density functions are shown in Figure 1.

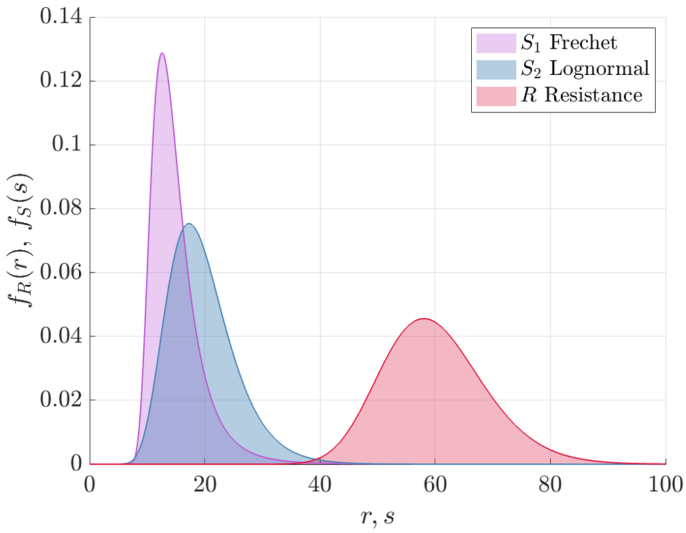

Figure 1. Definition of the illustrative problem. The performance function is $g(r, s_i) = r - s_i$. The resistance R is lognormal, while the two alternative load models are S_1, modeled by a generalized extreme value distribution, and S_2, modeled by a lognormal distribution. The two load models are calibrated to give the same probability of failure.

The two models are calibrated so that

$$\mathbb{P}[g(R, S_1) \leq 0] = \mathbb{P}[g(R, S_2) \leq 0] = 2.4501 \times 10^{-4}. \tag{40}$$

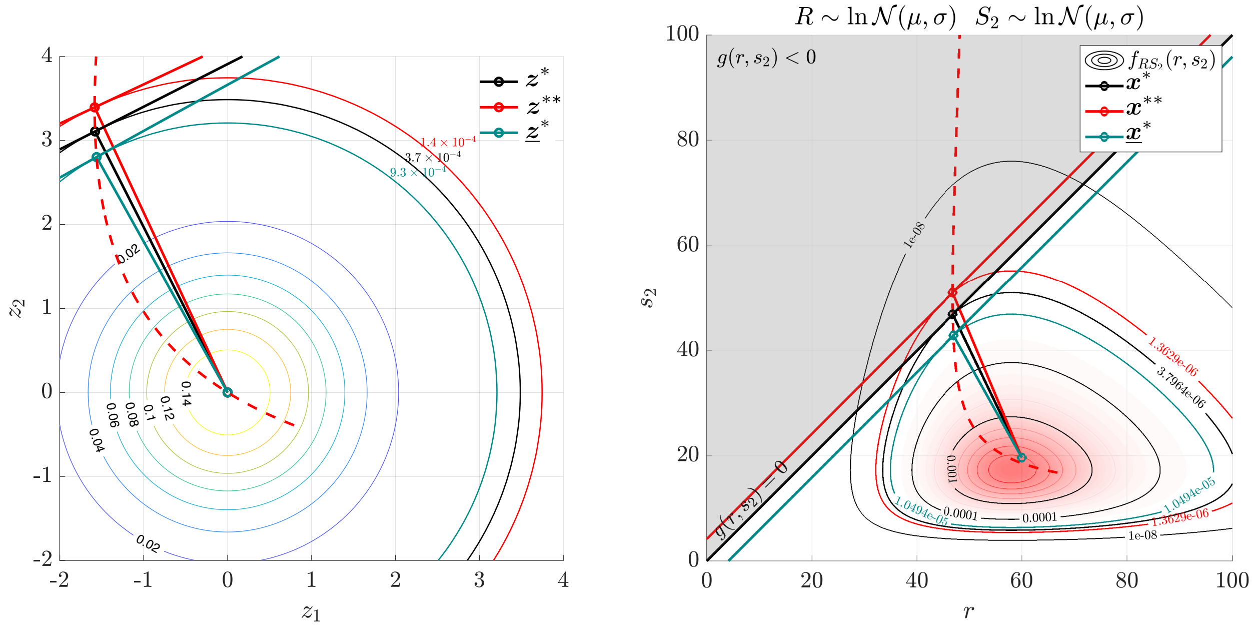

Figure 2. Comparison of the classical design point, the Mean Failure Point, and the Buffered Probable Point for the second system, in which the load is modeled by a lognormal distribution. The left panel refers to the standard normal space, while the right panel refers to the original physical space.

Consequently, the generalized reliability index is identical for the two systems,

$$\beta = -\Phi^{-1}(2.4501 \times 10^{-4}) = 3.4862. \tag{41}$$

According to the classical scalar reliability description, the two systems are therefore equivalent. This is precisely the situation targeted by the proposed framework: the probability of entering the failure domain is the same, but the distribution of the adverse tail and the corresponding representative failure configurations need not be the same.

Figure 2 and Figure 3 show the comparison in both the standard normal space and the original physical space of the two load cases. In each left panel, the black point denotes the classical design point $\boldsymbol{z}^*$, the red point denotes the Mean Failure Point $\boldsymbol{z}^{**}$, and the green point denotes the Buffered Probable Point $\underline{\boldsymbol{z}}^*$. The same notation is used for the corresponding points, $\boldsymbol{x}$, in the original space (right panels). The red level set represents the expected-failure level $G(\boldsymbol{z}) = \underline{y}$, while the green level set represents the buffered level $G(\boldsymbol{z}) = \bar{y}$. The classical limit-state surface $G(\boldsymbol{z}) = 0$, or equivalently $g(r, s_i) = 0$, remains the boundary between the safe and failure domains. The dashed red line represents the trace of the design points for different level sets.

For the GEV load model, the tail-dependent descriptors are

$$\underline{\beta} = \|\underline{\boldsymbol{z}}^*\| = 3.1940, \qquad \beta = 3.4862, \qquad \|\boldsymbol{z}^{**}\| = 3.7687.$$

For the lognormal load model, the corresponding values are

$$\underline{\beta} = \|\underline{\boldsymbol{z}}^*\| = 3.2083, \qquad \beta = 3.4862, \qquad \|\boldsymbol{z}^{**}\| = 3.7463.$$

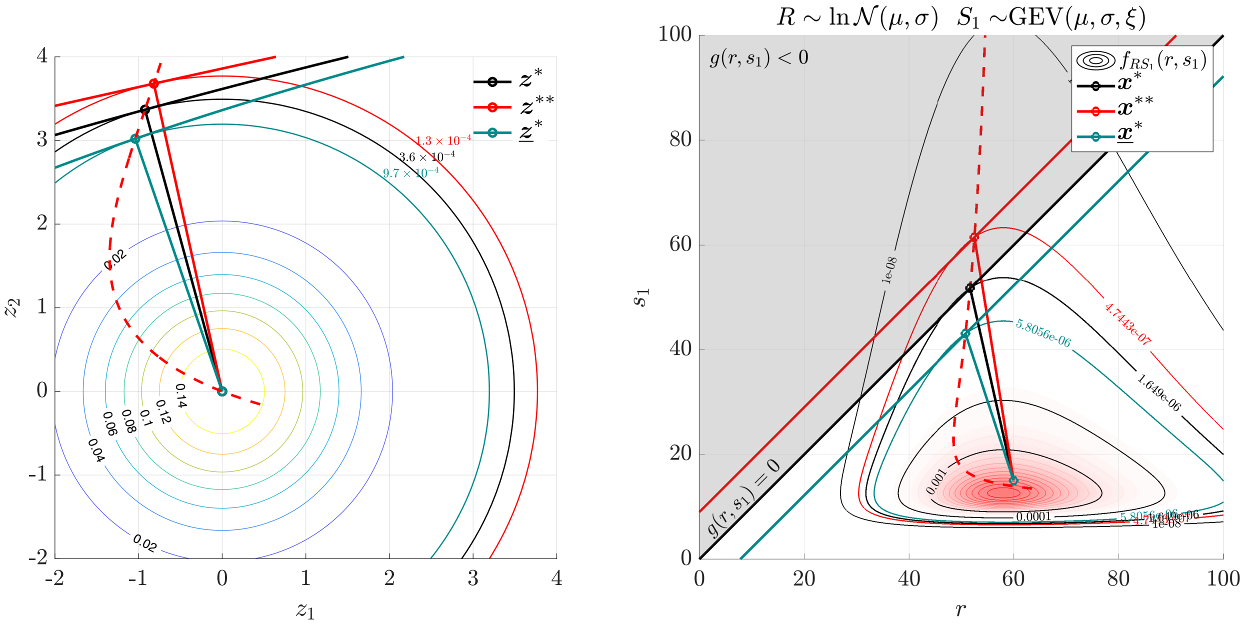

Figure 3. Comparison of the classical design point, the Mean Failure Point, and the Buffered Probable Point for the first system, in which the load is modeled by a GEV distribution. The left panel refers to the standard normal space, while the right panel refers to the original physical space.

The two systems therefore have the same generalized reliability index, but different buffered reliability indices and different Mean Failure Point norms. The GEV load model has a smaller BRI and a larger MFP norm than the lognormal load model. It follows that the two systems are not equivalent once the tail behavior of the performance function is considered.

Taken together, Figures 3 and 2 show that equality of $P_{\mathcal{F}}$ does not imply equality of the failure description. The classical index β assigns the same reliability to both systems, whereas the MFP and the BRI distinguish their representative failure states and adverse tails. In this example, the GEV load model leads to a more severe tail-dependent failure description than the lognormal load model. Therefore, in a reliability ranking that accounts for both likelihood and severity of failure, the system with lognormal load is safer, while the system with GEV load comes second despite having the same classical probability of failure. This simple resistance-load example captures the central message of the paper: equal failure probabilities need not imply equal reliability when reliability is interpreted as a statement about the mechanism and severity of failure. The proposed MFP and BRI reveal information that is hidden by the classical reliability index.

6. Concluding remarks

This paper revisited a basic convention of structural reliability: the identification of reliability with failure probability, or equivalently with the generalized reliability index. Although this convention is mathematically clear and computationally useful, it does not distinguish between systems that fail in different ways after entering the failure domain. This limitation becomes important whenever the objective of design is not merely to reduce the likelihood of failure, but also to control the mechanism and severity of failure. The proposed framework supplements the classical descriptor with two additional quantities. The Mean Failure Point identifies a representative failure configuration in the standard normal space. It is associated with the conditional expected performance within the failure domain and therefore lies beyond the classical limit-state surface. The Buffered Reliability Index is derived from the buffered probability of failure and provides a scalar measure of reliability that is sensitive to the adverse tail of the performance function. Together, the triplet $(P_{\mathcal{F}}, \boldsymbol{z}^{**}, \underline{\beta})$ gives a more complete reliability description. The probability of failure measures how likely failure is. The MFP indicates how the system is expected to fail. The BRI measures how severe the failure tail is in reliability-index form. In the linear standard normal case, these quantities admit closed-form expressions involving the standard normal hazard rate, which clarifies their relationship with the classical reliability index. In nonlinear structural systems, their separation may reveal mechanically meaningful differences hidden by $P_{\mathcal{F}}$ alone. The proposed quantities are not intended to replace the classical design point. Rather, they extend its interpretation. The design point remains the natural descriptor of incipient failure, while the MFP and BRI describe failure beyond the boundary. This shift is consistent with performance-based design, where the aim is not only to avoid failure, but also to understand and control the path and consequences of failure.

References

Breitung, K.: 1984, 'Asymptotic Approximations for Multinormal Integrals'. *Journal of Engineering Mechanics* **110**(3), 357–366.

Broccardo, M. and J. O. Royset: 2025, 'Tail-sensitive design point and reliability index: A refined approach to structural reliability design and assessment'. Presentation, JCSS Workshop, Tongji University. Available in the IRIS repository of the University of Trento.

Byun, J.-E. and J. O. Royset: 2022, 'Data-Driven Optimization of Reliability Using Buffered Failure Probability'. *Structural Safety* **98**, 102232.

Der Kiureghian, A.: 2022, *Structural and System Reliability.* Cambridge: Cambridge University Press, 1 edition.

Der Kiureghian, A., H.-Z. Lin, and S.-J. Hwang: 1987, 'Second-Order Reliability Approximations'. *Journal of Engineering Mechanics* **113**(8), 1208–1225.

Ditlevsen, O.: 1979, 'Generalized Second Moment Reliability Index'. *Journal of Structural Mechanics* **7**(4), 435–451.

Fréchet, M.: 1948, 'Les éléments aléatoires de nature quelconque dans un espace distancié'. *Annales de l'Institut Henri Poincaré* **10**(4), 215–310.

Hasofer, A. M. and N. C. Lind: 1974, 'An Exact and Invariant First-Order Reliability Format'. *Journal of the Engineering Mechanics Division* **100**(EM1), 111–121.

Karcher, H.: 1977, 'Riemannian Center of Mass and Mollifier Smoothing'. *Communications on Pure and Applied Mathematics* **30**(5), 509–541.

Mafusalov, A. and S. Uryasev: 2018, 'Buffered Probability of Exceedance: Mathematical Properties and Optimization'. *SIAM Journal on Optimization* **28**(2), 1077–1103.

Rockafellar, R. T. and J. O. Royset: 2010, 'On Buffered Failure Probability in Design and Optimization of Structures'. *Reliability Engineering & System Safety* **95**(5), 499–510.

Royset, J. O.: 2025, 'Risk-adaptive approaches to stochastic optimization: A survey'. *SIAM Review* **67**(1), 3–70.